Charge fluctuations in the unconventional metallic state of $Li_{0.9}Mo_6O_{17}$

J. Merino[1] and J. V. Alvarez[2]

[1]*Departamento de Física Teórica de la Materia Condensada, Condensed Matter Physics Center (IFIMAC) and Instituto Nicolás Cabrera, Universidad Autónoma de Madrid, Madrid 28049, Spain*

[2]*Departamento de Física de la Materia Condensada, Condensed Matter Physics Center (IFIMAC) and Instituto Nicolás Cabrera, Universidad Autónoma de Madrid, Madrid 28049, Spain*

(Received 17 June 2014; revised manuscript received 11 January 2015; published 29 January 2015)

Charge fluctuations in the quasi-one-dimensional material $Li_{0.9}Mo_6O_{17}$ are analyzed based on a multiorbital extended Hubbard model. A charge-ordering transition induced by Coulomb repulsion is found with a particular charge-ordering pattern. The metallic phase is characterized by the presence of a charge collective mode which softens signaling the proximity to the charge order transition. We argue that the scattering between electrons mediated by these charge fluctuations can lead to non-Fermi liquid behavior in a quasi-one-dimensional system consistent with the unconventional metallic behavior observed above the superconducting transition in $Li_{0.9}Mo_6O_{17}$.

DOI: 10.1103/PhysRevB.91.035135 PACS number(s): 71.10.Hf, 71.10.Fd, 74.40.Kb, 74.70.Kn

I. INTRODUCTION

Charge-ordering phenomena are relevant to a wide range of strongly correlated materials including copper-oxide (high-temperature) superconductors [1–5], manganites [6], sodium cobaltates [7], and the layered quarter-filled organic molecular conductors [8]. In particular, for the cuprate superconductors charge ordering has been found in the pseudogap region in close proximity to the superconducting phase raising questions about its relevance to the high-T_c superconductivity [9].

The purple bronze $Li_{0.9}Mo_6O_{17}$ is a quasi-one-dimensional material which displays behavior consistent with a Luttinger liquid (LL) [10–12] in a wide temperature range. When temperature is decreased an upturn of the resistivity occurs at $T_m \sim 20$ K and the material becomes superconducting at lower temperatures around $T_c \sim 1$ K [13]. The rather small enhancement of the resistivity below T_m (just a factor of 2) and the lack of spectral evidence of a gap makes it difficult to reconcile this upturn with an insulating phase. The fact that the resistivity is a decreasing function of temperature above the superconducting transition is in contrast with the superconducting transition in conventional metals but is also observed in quarter-filled organic materials [14,15]. Understanding the unconventional metallic state, whether it is a "bad" metal with incoherent excitations or not, may be crucial to the mechanism of superconductivity in $Li_{0.9}Mo_6O_{17}$.

Conventional charge density waves (CDWs) in solids involve a modulation of the electronic density accompanied by a crystal structure distortion. In $Li_{0.9}Mo_6O_{17}$ the resistivity upturn below T_m is not accompanied by a structural transition as evidenced by high-resolution x-ray scattering, neutron scattering [16], and thermal expansion [17] experiments. However, observing a structural instability driven by Fermi surface nesting requires a sufficiently large electron-lattice coupling which may not be present in $Li_{0.9}Mo_6O_{17}$ as observed in other systems such as quasi-one-dimensional TMTTF organic salts [18] or iron-based superconductors [19].

Here we present a microscopic theory for the unconventional metallic properties observed in $Li_{0.9}Mo_6O_{17}$. Based on a minimal extended Hubbard model recently introduced [20,21] we show that $Li_{0.9}Mo_6O_{17}$ is close to a charge-ordering (CO) transition driven by the Coulomb repulsion. Using the random phase approximation (RPA), we identify the CO pattern characterized by the ordering wave vector $\mathbf{Q}$, which can be different from a conventional $2k_F$ CDW. We obtain the typical temperature scale in the metal close to CO around which charge fluctuations are significant. The dynamical charge susceptibility displays a collective mode softening at momentum $\mathbf{Q}$ signaling the proximity to CO. We propose measurements of the dielectric constant [22], scanning tunneling microscopy (STM) [23], nuclear magnetic resonance (NMR) relaxation rate, $1/T_1T$, and quadrupolar relaxation rate [24] to probe the T dependence, strength, and CO pattern of charge fluctuations in $Li_{0.9}Mo_6O_{17}$, testing our predictions. The charge collective mode in the metallic phase can be explored with resonant inelastic x-ray scattering (RIX). In analogy with the effect of magnetic fluctuations in nearly antiferromagnetic metals, charge fluctuations can also lead to the unconventional T dependence of the specific-heat coefficient [13] and resistivity [12,25] observed in $Li_{0.9}Mo_6O_{17}$ assuming that the material is in proximity but not necessarily at CO.

II. MODEL

In Fig. 1 we show the zigzag ladders consisting of Mo and O atoms which lead to the characteristic quasi-one-dimensional electronic structure of the material. The minimal strongly correlated model which can capture the essential physics of $Li_{0.9}Mo_6O_{17}$ is a multiorbital extended Hubbard model [20] which reads

$$H = H_0 + H_U, \tag{1}$$

where H_0 is the noninteracting tight-binding Hamiltonian $H_0 = \sum_{i\alpha,j\beta} t_{i\alpha,j\beta}(d^\dagger_{i\alpha\sigma}d_{j\beta\sigma} + \text{c.c.})$, where $d^\dagger_{i\alpha\sigma}$ creates an electron with spin σ in a d_{xy} orbital of a Mo atom, α, which runs over four Mo atoms inside the unit cell of the crystal denoted by i which is shown in Fig. 1. The one-electron Hamiltonian can be expressed in terms of Bloch waves: $H_0 = \sum_{\mathbf{k}\alpha\beta\sigma} t_{\alpha\beta}(\mathbf{k})d^\dagger_{\mathbf{k}\alpha\sigma}d_{\mathbf{k}\beta\sigma}$ with the following nonzero matrix elements [20]: $t_{12}(\mathbf{k}) = t_{34}(\mathbf{k}) = -t_\perp e^{i\mathbf{k}\cdot\delta_\perp}$,

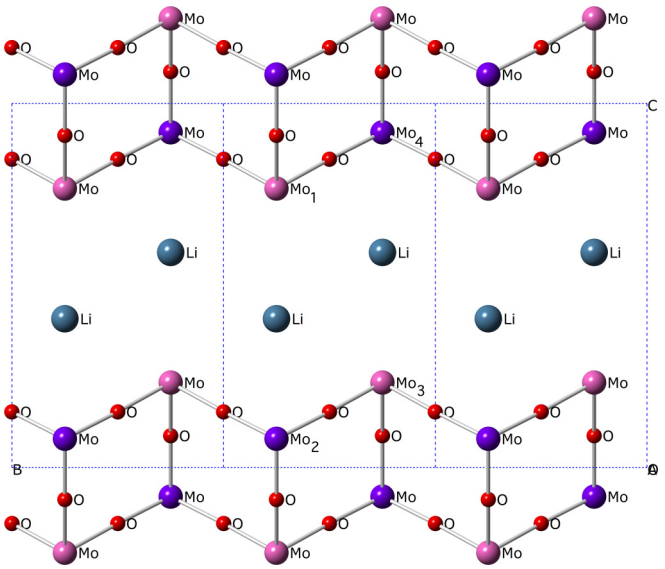

FIG. 1. (Color online) Charge-ordering phenomena in the extended Hubbard model (1) for $Li_{0.9}Mo_6O_{17}$. We show the crystal structure of $Li_{0.9}Mo_6O_{17}$ projected onto the b-c plane showing only the Mo and O atoms forming the zigzag ladders relevant to the low-energy electronic properties. The real-space charge-ordering pattern consisting of alternating charge-rich (purple) and charge-poor (magenta) Mo atoms arising in the U-V model is also shown.

$t_{13}(\mathbf{k}) = -2t' e^{i\mathbf{k}\cdot\delta_1}\cos(\frac{\mathbf{k}\cdot\mathbf{b}}{2})$, $t_{14}(\mathbf{k}) = -2tA(k_a,k_c)\cos(\frac{\mathbf{k}\cdot\mathbf{b}}{2})$, $t_{23}(\mathbf{k}) = -2tA(k_a,k_c)\cos(\frac{\mathbf{k}\cdot\mathbf{b}}{2})$, where $A(k_a,k_c) = e^{-i2\pi[0.1602k_a+0.1542k_c]}$, $\delta_\perp = 0.17\mathbf{a} - 0.31\mathbf{c}$, and $\delta_1 = 0.01\mathbf{a} + 0.53\mathbf{c}$. The momentum is expressed in terms of the reciprocal vectors, (a^*,b^*,c^*), of the unit cell coordinate system: $\mathbf{k} = k_a\mathbf{a}^* + k_b\mathbf{b}^* + k_c\mathbf{c}^*$, and the hopping parameters are taken as $t = 0.5$ eV, between the nearest-neighbor $Mo_1 - Mo_4$ and $Mo_2 - Mo_3$ atoms along a chain, $t_\perp = -0.024$ eV between $Mo_1 - Mo_2$ or $Mo_3 - Mo_4$ atoms in a rung of a ladder and $t' = 0.036$ eV between $Mo_1 - Mo_3$ atoms in neighboring zigzag ladders (see Fig. 1). The diagonalized Hamiltonian $H_0 = \sum_{\mathbf{k}\mu\sigma}\epsilon_\mu(\mathbf{k})d^\dagger_{\mathbf{k}\mu\sigma}d_{\mathbf{k}\mu\sigma}$ leads to four bands denoted by μ, the two lowest ones crossing the Fermi energy [20,26]. The Fermi surface close to one quarter filling, $n = 0.45$, is shown in Fig. 2(a).

The Coulomb interaction terms in the Hamiltonian have been described previously in [20,21] and read

$$H_U = \sum_{i\alpha,j\beta} U^{i\alpha j\beta}_{i\alpha j\beta} n_{i\alpha} n_{j\beta}. \tag{2}$$

This term only includes the density-density Coulomb interaction contributions included in the extended Hubbard model. The Coulomb matrix elements in momentum space, $U^{\gamma\delta}_{\alpha\beta}(\mathbf{q}) = U^{\alpha\beta}_{\alpha\beta}(\mathbf{q})\delta_{\alpha\gamma}\delta_{\beta\delta}$, have analogous expressions to the hopping terms but with the diagonal Coulomb energies, $U^{\alpha\alpha}_{\alpha\alpha}(\mathbf{q}) = U/2$. Here, we consider the nearest-neighbor Coulomb interactions with $V = V_\perp$ within the zigzag ladders which we name the U-V model and leads to the CO pattern in Fig. 1. The effect of next-nearest, V', and third-nearest neighbors, V'', relevant [20] to $Li_{0.9}Mo_6O_{17}$ is also analyzed.

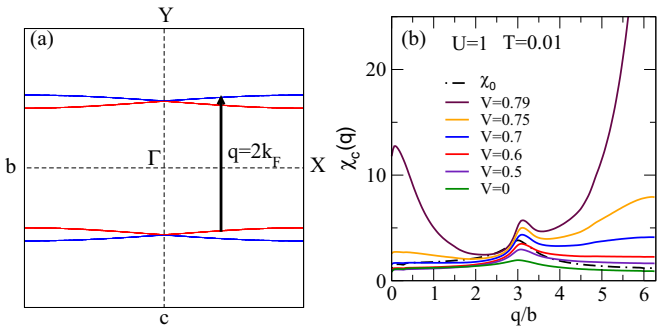

FIG. 2. (Color online) Charge order instability induced by Coulomb repulsion in the U-V model. (a) The Fermi surface obtained from our effective model for $Li_{0.9}Mo_6O_{17}$ is shown. (b) The static charge susceptibility $\chi_c(\mathbf{q})$ along the $(0,\frac{q}{b},\frac{\pi}{c/2})$ direction shows the rapid increase of charge fluctuations at wave vector $\mathbf{Q} = (0,\frac{\pi}{b/2},\frac{\pi}{c/2})$ associated with the Coulomb-induced CO occurring at $V_{CO} \approx 0.8$ eV. The smaller structure at $\mathbf{q} = (0,\frac{\pi}{b},\frac{\pi}{c/2})$ is related to Fermi surface nesting at $q = 2k_F \lesssim \pi/b$. All energies are given in eV.

III. MULTIORBITAL RPA APPROACH

The above model is analyzed based on a multiorbital random phase approximation (RPA) approach. The RPA charge susceptibility reads [27]

$$(\chi_c)^{np}_{lm}(\mathbf{q},i\omega) = (\chi_0)^{np}_{lm}(\mathbf{q},i\omega) - \sum_{uvwz}(\chi_c)^{np}_{uv}(\mathbf{q},i\omega) \times (U_c)^{uv}_{wz}(\mathbf{q})(\chi_0)^{wz}_{lm}(\mathbf{q},i\omega), \tag{3}$$

where the indices l,m,n,p refer to the four Mo d_{xy} orbitals present in the unit cell. $\hat{U}_c(\mathbf{q})$ is the Coulomb matrix appearing in Eq. (2) expressed in momentum space. The noninteracting susceptibility χ_0 reads

$$(\chi_0)^{wz}_{lm}(\mathbf{q},i\omega) = -\frac{2}{N}\sum_{\mathbf{k},\mu,\nu}\frac{a^l_\mu(\mathbf{k})a^{w*}_\mu(\mathbf{k})a^m_\nu(\mathbf{k}+\mathbf{q})a^{z*}_\nu(\mathbf{k}+\mathbf{q})}{i\omega + \epsilon_\nu(\mathbf{k}+\mathbf{q}) - \epsilon_\mu(\mathbf{k})} \times [f(\epsilon_\nu(\mathbf{k}+\mathbf{q})) - f(\epsilon_\mu(\mathbf{k}))], \tag{4}$$

where N is the number of lattice sites, and ν,μ are band indices. The matrix elements $a^l_\mu(\mathbf{k}) = \langle l|\mu\mathbf{k}\rangle$ are the coefficients of the eigenvectors diagonalizing H_0.

In Fig. 2 we show the evolution of the static RPA charge susceptibility obtained from $\chi_c(\mathbf{q}) = \sum_{uw}(\chi_c)^{uu}_{ww}(\mathbf{q},i0^+)/2$, with the nearest-neighbors Coulomb repulsion V and $U = 1$ eV for the pure U-V model. The susceptibility is evaluated along the $(0,\frac{q}{b},\frac{\pi}{c/2})$ direction in momentum space. The charge susceptibility is enhanced with V particularly at the wave vector $\mathbf{Q} = (0,\frac{\pi}{b/2},\frac{\pi}{c/2})$, which corresponds to having alternating charge-rich and charge-poor Mo atoms shown in Fig. 1. This signals the charge-ordering transition associated with the Coulomb repulsion (note that the unit cell defined by a,b,c contains four Mo atoms). There is a smaller structure at about $(0,\frac{\pi}{b},\frac{\pi}{c/2})$ associated with the nesting vector $2k_F$ connecting the different sections of the Fermi surface as shown in Fig. 2.

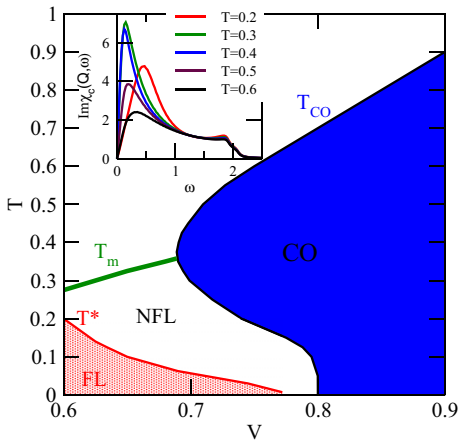

FIG. 3. (Color online) Phase diagram of the effective extended Hubbard U-V model for $Li_{0.9}Mo_6O_{17}$. The T-V phase diagram obtained from RPA is shown for fixed value of $U = 1$ eV and varying V. Charge-ordered (CO) and homogeneous metallic phases are separated by the CO transition line, T_{CO}, which displays "reentrant" behavior. T_m is the temperature scale associated with the onset of charge fluctuations. Fermi liquid (FL) and non-Fermi-liquid (NFL) phases are separated by the crossover scale T^*. The inset shows the T dependence of $\mathrm{Im}\chi_c(\mathbf{Q},\omega)$ in the metallic phase close to CO displaying the softening and enhancement of the charge collective mode around T_m. All energies are given in eV.

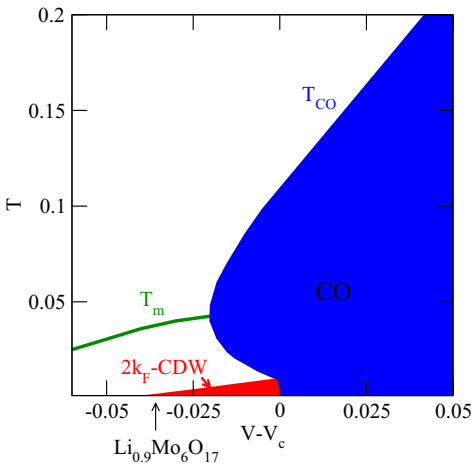

FIG. 4. (Color online) Phase diagram of an extended Hubbard model including up to the third-neighbor Coulomb interactions relevant for $Li_{0.9}Mo_6O_{17}$. The T-V phase diagram obtained from RPA is shown for fixed value of $U = 2$ eV and varying V for the model including up to third-nearest-neighbor Coulomb interactions. The phase diagram shows similar qualitative behavior to that in Fig. 3 with suppressed energy scales due to CO frustration effects. We also show here the low-temperature $2k_F$-type of instability occurring at low temperatures. The critical value for the CO driven by Coulomb repulsion is $V_c = 0.66$ as $T \to 0$. The suggested location for $Li_{0.9}Mo_6O_{17}$ at ambient pressure is marked with a vertical arrow. The system would effectively shift away from the CO transition under pressure. All energies are given in eV.

A. Phase diagram

The T-V phase diagram for this U-V model is shown in Fig. 3 for $U = 1$ eV. The metallic and charge-ordered (CO) phases are separated by a "reentrant" charge-ordering transition line T_{CO}. Such "reentrant" behavior is consistent [28] with previous studies of the quarter-filled extended Hubbard model using FLEX [29] and its extensions with vertex corrections [30] DMFT [31] and exact diagonalization [32]. In the metallic phase close to CO, where $Li_{0.9}Mo_6O_{17}$ is presumably located, charge fluctuations with $\mathbf{Q} = (0,\pi/(b/2),\pi/(c/2))$ are strongly enhanced (see inset of Fig. 3). A large enhancement of low-energy spectral weight occurs signaling the formation of a charge collective mode which softens and increases in amplitude with decreasing T. Such T dependence of the charge collective mode occurs down to T_m. At this temperature such behavior is reversed; i.e., the collective mode hardens following the "reentrant" shape of the transition line T_{CO}. Thus T_m sets the temperature scale at which charge fluctuations associated with the Coulomb repulsion are significant even if no "reentrance" is present in the phase diagram.

Based on our previous derivation of the microscopic model [20] for $Li_{0.9}Mo_6O_{17}$ we have extended Coulomb interactions up to third-nearest-neighbors taking $V' = 0.7V$ and $V'' = 0.66V$. The corresponding phase diagram for fixed $U = 2$ is shown in Fig. 4. The metallic and charge-ordered (CO) phases are separated by a "reentrant" charge-ordering transition line T_{CO} similar to the U-V model in Fig. 3. In the metallic phase in proximity to T_{CO} charge fluctuations become strongest at the temperature scale, T_m. The main effect of V' and V'' is a different CO pattern and strong suppression of T_{CO} and T_m with respect to the U-V model. This suppression can be attributed to the CO frustration effects introduced by longer range Coulomb repulsion. At low temperatures below the "reentrance" region a $2k_F$-CDW type of instability with $\mathbf{Q} = (0,2k_F,2\pi/c)$ is favored by V''.

We note that the CO pattern for the extended Hubbard model, i.e., up to third-nearest-neighbor interactions, differs from the one illustrated in Fig. 1. In fact at low temperatures $\mathbf{Q} \approx (0,\pi/b,2\pi/c)$ is of the type of the $2k_F$-CDW instability, i.e., with an electronic modulation of four lattice spacings (the distance between sites in the chains is $b/2$ in $Li_{0.9}Mo_6O_{17}$). This is because in the present parameter regime in which $V = 1.51V'' < 2V''$, electron configurations in which two neighbor charge-rich sites alternate with two neighbor charge-poor sites along a chain are stabilized. This is consistent with Hubbard [33] predictions for quarter-filled Wigner chains in which the convexity condition of the potential is violated. Hence, the present $\mathbf{Q} \approx (0,\pi/b,2\pi/c)$ CO pattern induced by longer range Coulomb repulsion can be relevant to $Li_{0.9}Mo_6O_{17}$ instead of the checkerboard pattern shown in Fig. 1. The enhancement of a $2k_F$-type of CO instability induced by long-range Coulomb interaction has been discussed in the context of quasi-one-dimensional organic materials [34].

Close to the CO instability, electron scattering mediated by dynamical charge fluctuations [35] influences normal metallic properties. In analogy with nearly antiferromagnetic two-dimensional metals the scattering rate displays NFL behavior, $1/\tau(T) \propto T$, above T^* crossing over [36] to FL behavior $1/\tau(T) \propto T^2$ below T^* (as obtained in Ref. [36] and shown in Fig. 3). We expect that the particular T dependence of charge fluctuations found here will lead to characteristic

resistivity and specific-heat slope [13] enhancements around T_m. Furthermore, we find that the phase diagrams in Figs. 3 and 4 agree qualitatively with key features of $Li_{0.9}Mo_6O_{17}$. Experiments under an external pressure [13,20] show how the temperature for the resistivity upturn, T_m, is suppressed [25], and T^* increases (see Fig. 3) stabilizing the FL state. This is consistent with the phase diagram shown in Fig. 4, since applying pressure is equivalent to driving the system into the metallic phase. Since RPA overestimates broken-symmetry states, renormalization due to feedback effects of the CO fluctuations and electron localization will strongly suppress [30] our T_{CO} and T_m bringing them closer to experimental values.

B. Charge collective mode

In Fig. 5 we analyze $\mathrm{Im}\chi_c(\mathbf{q},\omega)$ as the system is driven close to CO at low temperatures, $T = 0.05$, in the U-V model. For noninteracting electrons, $U = V = 0$, spectral weight is found in the particle-hole continuum with small weight in the region between 0 and $2k_F$ as expected for quasi-one-dimensional systems. Once the on-site Coulomb repulsion is turned on spectral weight is enhanced around the highest energy branch of the particle-hole continuum due to particle-hole excitations promoted by U. As V is increased a redistribution of charge spectra around $\mathbf{Q}$ occurs in which particle-hole excitations of lower and lower energies gain weight. At $V = 0.68$ a collective charge fluctuation mode is clearly resolved. Close to the CO transition, $V \lesssim V_{CO}$, the collective mode amplitude increases shifting to zero energy signaling the Coulomb-driven CO transition. The behavior found for $\mathrm{Im}\chi_c(\mathbf{q},\omega)$ close to CO can be understood from the

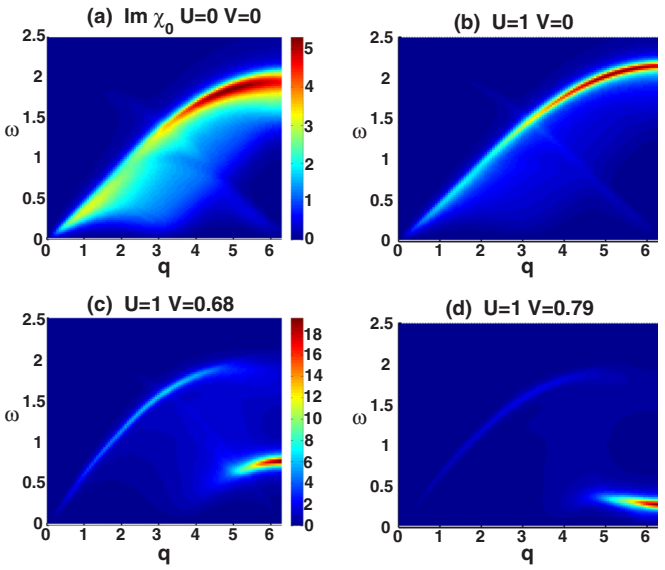

FIG. 5. (Color online) Imaginary part of the charge susceptibility $\mathrm{Im}\chi_c(q,\omega)$ of the U-V model showing the emergence and softening of the collective excitation as the interaction increases. (a) Noninteracting charge susceptibility $\mathrm{Im}\chi_0(q,\omega)$ displaying the particle-hole continuum, (b) a Hubbard-like interaction ($U = 1$ eV, $V = 0$), (c) an interaction compatible with purple bronze phenomenology $U = 1$ eV, $V = 0.68$ eV, and (d) close to the CO transition $U = 1, V = 0.79$ eV. Temperature is $T = 0.05$ eV. All energies are given in eV.

singular part of the charge susceptibility in a two-dimensional system: $\chi_c(\mathbf{q},\omega) \approx \frac{A}{i\omega-\omega_{\mathbf{q}}}$, with $\omega_{\mathbf{q}} = \omega_0 + C|\mathbf{q}-\mathbf{Q}|^2$, where $\omega_0 \to 0$ as the CO boundary is approached [35] and C is a positive constant.

The dynamical charge response of the system, $\mathrm{Im}\chi_c(\mathbf{q},\omega)$, can be experimentally analyzed using RIX. In particular, the dispersion of the collective mode discussed above around $\mathbf{Q}$ could be extracted probing the proximity of the system to CO. Analogous plasmon softening around $2k_F$ has been observed with inelastic electron scattering on materials driven close to a conventional charge density wave [37] instability. Measurements of the real part of the dielectric constant of the material could also track the enhancement of charge fluctuations around the resistivity upturn as observed in quasi-one-dimensional organic systems [22].

IV. CONNECTION WITH LUTTINGER LIQUID BEHAVIOR

There is extensive experimental evidence showing that $Li_{0.9}Mo_6O_{17}$ behaves as a Luttinger liquid at high temperatures above T_m. The crossover temperature scale, T_{LL}, at which the crossover from one-dimensional to three-dimensional metal occurs has been studied (see for instance [38]) in the past. We first obtain various estimates that are relevant to $Li_{0.9}Mo_6O_{17}$. Assuming $t_\perp = 0.03$ eV, different available estimates of T_{LL} would predict $T_{LL} \sim t_\perp/\pi = 0.01$ eV (Fermi surface warping), $t_\perp \sim (\frac{t_\perp}{t})^{\frac{1}{1-\alpha}} \sim 0.0002$ eV (weak-coupling RG [39]), and $T_{LL} \sim t_\perp/2/\pi \sim 0.005$ eV (chain-DMFT [40]) suggesting that the Luttinger liquid survives to very low temperatures. Since the RPA greatly overestimates T_{CO} and consequently T_m it is then possible that T_m is smaller than T_{LL} (as experimentally observed) when renormalization effects are properly taken into account.

In order to study the dimensional crossover specific to the present system, we consider model (1) and start from the limit of decoupled ladders. We estimate T_{LL} using the RG expression for $T_{LL} = t(\frac{t_\perp}{t})^{1/(1-\alpha)}$ (i.e., the most LL favoring of the three) and a value of α given by

$$\alpha = \left(K_{\rho-} + K_{\rho-}^{-1} + K_{\rho+} + K_{\rho+}^{-1} - 4\right)/8. \tag{5}$$

The expressions used here are

$$K_{\rho\pm} = \sqrt{\frac{2\pi v_f \mp g_{\rho\pm}}{2\pi v_f \pm g_{\rho\pm}}}, \tag{6}$$

where the couplings expressed as a function of the model microscopic interactions are

$$\begin{aligned} g_{\rho+} &= U + V_\parallel[4 - \sin(\pi x)] + 2V_\perp + V'[4 + \sin(\pi x)], \\ g_{\rho-} &= V_\parallel \sin(\pi x) - V_\perp. \end{aligned} \tag{7}$$

Here $V_\parallel = V_\perp = V$ and $V' = 0.7V$. The system is assumed to be close to quarter filling and x is the doping. Note that we start from the quasi-one-dimensional limit but otherwise we are using the same microscopic model used to determine the phase diagram. Results for T_{LL} and α as a function of V are presented in Fig. 6. Note that the present weak-coupling RG analysis can predict LL exponents, α, consistent with ARPES experiments using Hubbard parameters appropriate for $Li_{0.9}Mo_6O_{17}$. The corresponding T_{LL} can be of the same

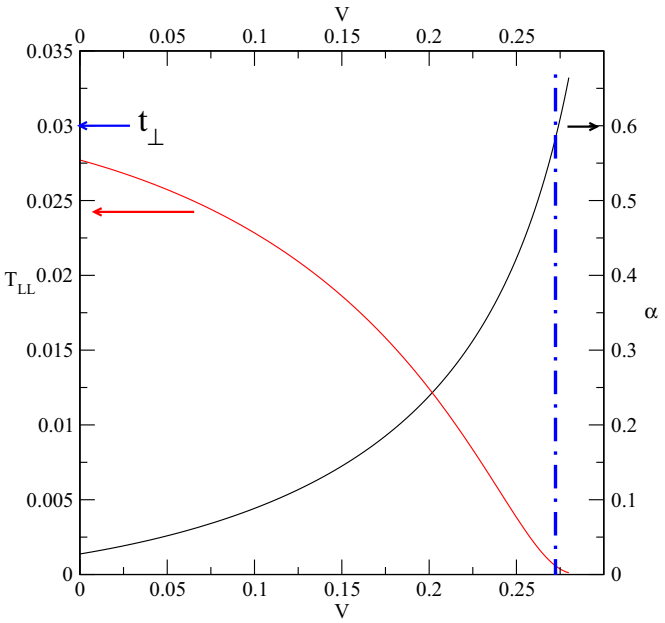

FIG. 6. (Color online) Crossover temperature T_{LL} and exponent of the density of states α estimated as a function of the coupling V.

order of magnitude as T_m. However, more sophisticated nonperturbative methods are needed to definitively draw conclusions about the predicted magnitude of T_{LL} in $Li_{0.9}Mo_6O_{17}$.

Finally, it is worth discussing the two different scenarios which can arise depending on the relative values of T_m and T_{LL} [38]. If $T_m > T_{LL}$, CO fluctuations modify the LL properties before entering the superconducting state directly from the LL. On the other hand if $T_m < T_{LL}$ then a crossover from the LL to a NFL dominated by the critical CO fluctuations occurs with lowering temperature, before superconductivity sets in at even lower temperatures below T_c. Our approach would be valid in the latter scenario in which Fermi liquid behavior occurs below T^*. In both scenarios the high-T LL behavior is modified by the charge fluctuations building in as T decreases until the system crosses over to NFL behavior characterized by the critical charge fluctuations. This NFL behavior is consistent with deviations from exact LL predictions found in ARPES experiments [10] at and below T_m. It is then an appealing open issue to analyze the effect of charge fluctuations in ARPES starting from the LL high-temperature regime and provide a unified picture merging the Hertz-Millis and quasi-one-dimensional quantum critical scenarios. However, this goes beyond the scope of the present work which mainly identifies the mechanism responsible for the unconventional metallic properties observed. Describing the crossover from the LL to the present NFL dominated by critical CO fluctuations requires more sophisticated theoretical tools than the RPA approach presented here.

V. CONCLUSIONS

We propose a framework to describe the anomalous metallic behavior of the quasi-one-dimensional $Li_{0.9}Mo_6O_{17}$ at temperatures $T \approx T_m$ around the resistivity upturn. The small resistivity enhancement accompanied with a weak feature on the specific heat are not consistent with an insulating state. There are neither signatures of a structural distortion nor convincing evidence of another phase transition. Our analysis shows that these anomalies can be attributed to strong CO fluctuations and manifest themselves through a low-energy collective excitation directly visible in RIX. CO fluctuations pinned by defects would also reveal themselves as a line broadening of NMR spectra in analogy to observations in cuprates [41] and $NbSe_2$ [42]. Our analysis suggests that $Li_{0.9}Mo_6O_{17}$ around T_m can be a realization of NFL behavior occurring between the high-temperature LL state and the low-temperature Fermi liquid (or broken-symmetry phase). Such NFL behavior is generic of quasi-one-dimensional systems close to CO quantum critical points.

ACKNOWLEDGMENTS

We acknowledge financial support from MINECO, MAT2012-37263-C02-01 (J.M.) and FIS2012-37549-C05-03 (J.V.A.).

[1] J. M. Tranquada, B. J. Sternlieb, J. D. Axe, Y. Nakamura, and S. Uchida, Nature (London) **375**, 561 (1995).
[2] T. Wu, H. Mayaffre, S. Kramer, M. Horvatic, C. Berthier, W. N. Hardy, R. Liang, D. A. Bonn, and M.-H. Julien, Nature (London) **477**, 191 (2011).
[3] G. Ghiringhelli *et al.*, Science **377**, 821 (2012).
[4] E. H. da Silva Neto *et al.*, Science **343**, 393 (2014).
[5] R. Comin *et al.*, Science **343**, 390 (2014).
[6] S. Mori, C. H. Chen, and S.-W. Cheong, Nature (London) **392**, 473 (1998).
[7] N. P. Ong and R. J. Cava, Science **305**, 52 (2004); M. L. Foo, Y. Wang, S. Watauchi, H. W. Zandbergen, T. He, R. J. Cava, and N. P. Ong, Phys. Rev. Lett. **92**, 247001 (2004).
[8] H. Seo, J. Merino, H. Yoshioka, and M. Ogata, J. Phys. Soc. Jpn. **75**, 051009 (2006).
[9] E. Fradkin and S. Kivelson, Nat. Phys. **8**, 864 (2012).
[10] F. Wang, J. V. Alvarez, S.-K. Mo, J. W. Allen, G.-H. Gweon, J. He, R. Jin, D. Mandrus, and H. Hochst, Phys. Rev. Lett. **96**, 196403 (2006); F. Wang, J. V. Alvarez, J. W. Allen, S.-K. Mo, J. He, R. Jin, D. Mandrus, and H. Hochst, *ibid.* **103**, 136401 (2009); L. Dudy, J. D. Denlinger, J. W. Allen, F. Wang, J. He, D. Hitchcock, A. Sekiyama, and S. Suga, J. Phys.: Condens. Matter **25**, 014007 (2013).
[11] J. Hager, R. Matzdorf, J. He, R. Jin, D. Mandrus, M. A. Cazalilla, and E. W. Plummer, Phys. Rev. Lett. **95**, 186402 (2005).
[12] N. Wakeham, A. F. Bangura, X. Xu, J.-F. Mercure, M. Greenblatt, and N. E. Hussey, Nat. Commun. **2**, 396 (2011).
[13] C. Schelenker, H. Schwenk, C. Escribe-Filippini, and J. Marcus, Physica B **135**, 511 (1985).
[14] N. Morinaka *et al.*, Phys. Rev. B **80**, 092508 (2009).

[15] S. Kaiser, M. Dressel, Y. Sun, A. Greco, J. A. Schlueter, G. L. Gard, and N. Drichko, Phys. Rev. Lett. **105**, 206402 (2010).
[16] M. S. da Luz, J. J. Neumeier, C. A. M. dos Santos, B. D. White, H. J. I. Filho, J. B. Leao, and Q. Huang, Phys. Rev. B **84**, 014108 (2011).
[17] C. A. M. dos Santos, B. D. White, Y. K. Yu, J. J. Neumeier, and J. A. Souza, Phys. Rev. Lett. **98**, 266405 (2007).
[18] D. S. Chow, F. Zamborszky, B. Alavi, D. J. Tantillo, A. Baur, C. A. Merlic, and S. E. Brown, Phys. Rev. Lett. **85**, 1698 (2000).
[19] A. K. Jasek, A. Blachowski, K. Ruebenbauer, Z. Bukowski, J. G. Storey, and J. Karpinski, J. Alloys Compd. **609**, 150 (2014).
[20] J. Merino and R. H. McKenzie, Phys. Rev. B **85**, 235128 (2012).
[21] P. Chudzinski, T. Jarlborg, and T. Giamarchi, Phys. Rev. B **86**, 075147 (2012).
[22] F. Nad, P. Monceau, C. Carcel, and J. M. Fabre, J. Phys.: Condens. Matter **12**, L435 (2000); P. Monceau, Adv. Phys. **61**, 325 (2012).
[23] C. J. Arguello, S. P. Chockalingam, E. P. Rosenthal, L. Zhao, C. Gutierrez, J. H. Kang, W. C. Chung, R. M. Fernandes, S. Jia, A. J. Millis, R. J. Cava, and A. N. Pasupathy, Phys. Rev. B **89**, 235115 (2014).
[24] A. Suter, M. Mali, J. Roos, and D. Brinkmann, Phys. Rev. Lett. **84**, 4938 (2000).
[25] C. Escribe-Filippini, J. Beille, M. Boujida, J. Marcus, and C. Schlenker, Physica C **162–164**, 427 (1989).
[26] Z. S. Popović and S. Satpathy, Phys. Rev. B **74**, 045117 (2006); M.-H. Wangbo and E. Canadell, J. Am. Chem. Soc. **110**, 358 (1988).
[27] S. Graser, T. A. Maier, P. J. Hirschfeld, and D. J. Scalapino, New J. Phys. **11**, 025016 (2009).
[28] In contrast, we note that such "reentrant" behavior would not occur in Hertz-Millis [43] theory and certain diagrammatic approaches [44]. Since there is no exact solution to the two-dimensional extended Hubbard model on a square lattice we cannot conclude on whether such reentrance exists or not in this model.
[29] K. Yoshimi, J. Phys. Soc. Jpn. **81**, 063003 (2012).
[30] K. Yoshimi, T. Kato, and H. Maebashi, J. Phys. Soc. Jpn. **78**, 104002 (2009).
[31] R. Pietig, R. Bulla, and S. Blawid, Phys. Rev. Lett. **82**, 4046 (1999); N. H. Tong, S. Q. Shen, and R. Bulla, Phys. Rev. B **70**, 085118 (2004).
[32] C. S. Hellberg, J. Appl. Phys. **89**, 6627 (2001).
[33] J. Hubbard, Phys. Rev. B **17**, 494 (1978).
[34] K. Kuroki and Y. Tanaka, J. Phys. Soc. Jpn. **74**, 1694 (2005).
[35] C. Castellani, C. Di Castro, and M. Grilli, Phys. Rev. Lett. **75**, 4650 (1995).
[36] J. Merino, A. Greco, N. Drichko, and M. Dressel, Phys. Rev. Lett. **96**, 216402 (2006); note the misprint in Eq. (3) of this paper where ω' should read ν, the integration variable.
[37] J. van Wezel, R. Schuster, A. König, M. Knupfer, J. van den Brink, H. Berger, and Bernd Büchner, Phys. Rev. Lett. **107**, 176404 (2011).
[38] T. Giamarchi, Chem. Rev. **104**, 5050 (2004).
[39] C. Bourbonnais and L. G. Caron, Physica B+C **143**, 450 (1986).
[40] S. Biermann, A. Georges, A. Lichtenstein, and T. Giamarchi, Phys. Rev. Lett. **87**, 276405 (2001).
[41] T. Wu, H. Mayaffre, S. Krämer, M. Horvatic, C. Berthier, W. N. Hardy, R. Liang, D. A. Bonn, and M.-H. Julien, arXiv:1404.1617.
[42] K. Ghoshray *et al.*, J. Phys.: Condens. Matter **21**, 155703 (2009).
[43] J. A. Hertz, Phys. Rev. B **14**, 1165 (1976); A. J. Millis, *ibid.* **48**, 7183 (1993).
[44] S. Andergassen, S. Caprara, C. Di Castro, and M. Grilli, Phys. Rev. Lett. **87**, 056401 (2001).